UNSTEADY HYDRODYNAMIC AND THERMAL BOUNDARY LAYERS OVER A FLAT PLATE WITH UNIFORM INJECTION OR SUCTION

Ihsan Y.Hussain
Mech. Engr. Dept.
College of Eng. / University of Baghdad
Baghdad-Iraq

Abdul Wahab A. Taha
Mech. Engr. Dept.
College of Eng. / University of Al-Mustansiriya
Baghdad-Iraq

Ayser M. Fleh
Mech. Engr. Dept.
College of Eng. / University of Baghdad
Baghdad-Iraq

ABSTRACT

A computational algorithm for calculating the unsteady compressible and turbulent hydrodynamic and thermal boundary layers over a porous flat plate with uniform suction or injection is developed in the present work. The mathematical modeling involves the derivation of the governing partial differential equations of the problem. These are the continuity, the momentum, the ($\kappa-\varepsilon$) turbulence model and the energy equations. Besides, the perfect gas law and the Sutherland's law of molecular viscosity are also used. A proper initial and boundary conditions are specified to be used in the solution of the governing equations. A numerical solution of the governing equations is made by using the control volume approach, with non-staggered grid technique and modified SIMPLE algorithm. The numerical solution is capable of calculating the velocity and temperature distributions of the calculation domain, the kinetic energy and dissipation of turbulence, the local and average skin-friction and heat transfer coefficients and Nusselt number, and the hydrodynamic and thermal boundary layers thicknesses. All these parameters are calculated at the transient and steady states. The numerical results show that the developed algorithm is capable of calculating the flow field, properly and accurately. The results show that injection causes slight decrease in the temperature inside the thermal boundary layer, a decrease in skin – friction coefficient, a slight increase in the Nusselt number, a decrease in hydrodynamic boundary layer thickness, an increase in thermal boundary layer thickness and an increase in the time required to reach the steady state. Suction almost causes reverse effects.

الخلاصة

في البحث الحالي، تم التوصل إلى نموذج رياضي عددي لحساب الطبقة المتاخمة الهيدروديناميكية والحرارية العابرة، الانضغاطية والمضطربة على صفيحة مسطحة مسامية مع حقن وسحب بسرعة منتظمة من الصفيحة. يتضمن النموذج الرياضي اشتقاق المعادلات التفاضلية الجزئية للمسألة، والتي هي معادلات الاستمرارية، الزخم، معادلتي نموذج ($\kappa-\varepsilon$) للاضطراب ومعادلة الطاقة. بالإضافة إلى ذلك، تم استخدام معادلة الغاز المثالي وقانون سذرلاند للزوجة الديناميكية. تم تعريف ظروف ابتدائية وحدية مناسبة لاستخدامها في حل المعادلات. تم حل المعادلات عدديا باستخدام تقنية الحجم المحكوم مع شبكة غير مزحفة وطريقة (SIMPEL) المعدلة. للحل العددي القابلية على حساب توزيعات السرع ودرجات الحرارة، الطاقة الحركية والتبدد للاضطراب،

القيم الموقعية والمتوسطة لمعدل الاحتكاك، معامل انتقال الحرارة ورقم نسلت، سمك الطبقة المتاخمة الهيدروديناميكية والحرارية. كل هذه المتغيرات تحسب للحالة العابرة والمستقرة. أظهرت النتائج العددية إن النموذج العددي الذي تم التوصل أليه له القابلية على حساب الجريان بصورة مناسبة ودقيقة. بينت النتائج العددية أن الحقن يسبب انخفاض طفيف في درجة الحرارة داخل الطبقة المتاخمة الحرارية, انخفاض في قيم معامل الاحتكاك, زيادة طفيفة في قيم رقم نسلت, انخفاض في سمك الطبقة المتاخمة الهيدروديناميكية, زيادة في سمك الطبقة المتاخمة الحرارية, وزيادة في الوقت المطلوب للوصول إلى الحالة المستقرة.

KEYWORDS

Boundary Layer, Flat Plate, Unsteady, Hydrodynamic and Thermal, Injection and Suction.

INTRODUCTION:-

The flow and heat transfer inside the boundary layer may be either steady or transient (unsteady) .The most important cases in practical applications are usually steady cases. Nevertheless, there exists some important unsteady applications, such as motion started from rest, periodic motion, accelerated motions, boundary layer behind a moving normal shock wave,…etc. Besides, all processes in nature must pass through a transient period before they attain the steady conditions. Therefore, the calculation of the transient phenomena associated with any process is an important matter. The development of the theory of boundary layer flow in compressible streams was stimulated by the progress in aeronautical engineering and rockets and artificial satellites. When flight velocities of the order of multiples of the velocity of sound are attained, the work of compression and energy dissipation produces considerable increase in temperature and always forces to include thermal boundary layer in the analysis, because the two boundary layers strongly interact with each other. Boundary layers with localized injection and section are frequently found in engineering applications, the configuanation is often found in gas turbine applications, where the aim is to protect the surface from high transfer rates. Other applications have been boundary layer control, drying processes in the chemical industry and more recently, cooling of electronics by means of injections through the printed circuit board. Most of these applications are concerned with injections through a series of small holes. However, many applications also exist (boundary layer control and high efficiency heat exchangers) where the injection is performed through a porous surface. The effects of wall suction or injection have been studied experimentally or numerically, for various flow fields. It has been known that in turbulent boundary layer, uniform blowing from the wall decreases the skin friction and increases the strength of fluctuating quantities, while suction has nearly the opposite effect. However, the increase of turbulent fluctuations from blowing may cause an increase of drag in the downstream due to strong turbulent motion there. In the case of suction, the downstream skin friction may be reduced due to the stabilization of turbulence even through the skin friction increases near the place of suction. The problem was investigated with different approaches. **(Jeongyoung and Haecheon. 1999)** investigated effect of uniform blowing or suction from aspanwise slot on a turbulent layer flow by using the direct numerical simulation technique. **(Per-Age and Anatoli 2000)** examined the effect of localized injection through porous strip on a turbulent boundary layer at zero pressure gradient condition experimentally. **(Park and Sung 2001)** performed study to analyze flow structure behind local suction and blowing in a flat plate turbulent boundary layer. **(Kyoungyoun and Haying 2001)** investigated the effects of local blowing or suction from a span wise on a turbulent boundary layer flow using the direct numerical simulation technique, where three different blowing or suction velocities are imposed on the slot keeping blowing or suction flow rate constant. **(Kyoungyoun and Hynng 2003)** performed direct numerical simulation to analyze the effect of, periodical blowing through a span wise slot on turbulent boundary layer. The present work deals with the calculation of the transient compressible turbulent hydrodynamic and thermal boundary layers over a porous flat plate with uniform suction

or injections see **Fig.1**. It will be assumed that the quantity of fluid removed from the stream is so small that only fluid particles in the immediate neighborhood of the wall are sucked (injected) a way. That is to say the ratio of suction or injection velocity $V_w\ (x)$ to free stream velocity U_∞ is small, say V_w/U_∞ =0.001 to 0.01 the condition of no slip at the wall is retained with suction present, as well as the expression $\tau_w = \mu\left(\frac{\partial u}{\partial y}\right)_0$ for the shearing stress at the wall

MATHEMATICAL MODELIN:-

The usual system of Cartesian coordinates will be adapted, the x-axis being along the wall, and the y-axis being at right angle to it. Suction or injection will be accounted for by prescribing non-zero normal velocity component (V_w) at the wall. In the case of suction Vw<0 and V_w>0 will be used for injection, see Fig (1). Flow and heat transfer with negligible edge effect are assumed ($w=0, \partial(\ )/\partial z = 0$) with uniform suction or injection and negligible axial diffusion ($\partial^2(\ )/\partial x^2 = 0$)

A cording to the previously mentioned assumptions, the governing conservation and constitution laws will be presented here interims of the geometry and coordinates system of **Fig.1** These are the continuity, the momentum, the (K-ε) turbulence model and the energy equations **(Ayser 2005)**:

The continuity equation is

$$\frac{\partial \rho}{\partial \tau} + \frac{\partial}{\partial x}(\rho u) + \frac{\partial}{\partial y}(\rho v) = 0 \qquad (1)$$

The x-direction momentum equations is

$$\rho\left(\frac{\partial u}{\partial \tau} + u\frac{\partial u}{\partial x} + v\frac{\partial u}{\partial y}\right) = -\frac{\partial P}{\partial x} + \frac{\partial}{\partial y}\left(\mu\frac{\partial u}{\partial y}\right) + \frac{\partial}{\partial y}\left(\mu_t\frac{\partial u}{\partial y}\right) \qquad (2)$$

The y-direction momentum equation is;

$$\rho\left(\frac{\partial v}{\partial t} + u\frac{\partial v}{\partial x} + v\frac{\partial v}{\partial y}\right) = -\frac{\partial P}{\partial y} + \frac{\partial}{\partial y}\left(\mu\frac{\partial v}{\partial y}\right) + \frac{\partial}{\partial y}\left(\mu_t\frac{\partial v}{\partial y}\right) \qquad (3)$$

The standard form of (K-ε) model is as follows:-
Turbulence kinetic energy equation;

$$\rho\left(\frac{\partial \kappa}{\partial t} + u\frac{\partial \kappa}{\partial x} + v\frac{\partial \kappa}{\partial y}\right) = \frac{\partial}{\partial y}\left(\frac{\mu_t}{\sigma\kappa}\frac{\partial \kappa}{\partial y}\right) + \mu_t\left(\frac{\partial u}{\partial y}\right)^2 - \rho\varepsilon \qquad (4)$$

And dissipation of turbulence kinetic energy equation;

$$\rho\left(\frac{\partial \varepsilon}{\partial t}+u\frac{\partial \varepsilon}{\partial x}+v\frac{\partial \varepsilon}{\partial y}\right)=\frac{\partial}{\partial y}\left(\frac{\mu_t}{\sigma\varepsilon}\frac{\partial \varepsilon}{\partial y}\right)+\mu_t c_{\varepsilon_1}\frac{\varepsilon}{\kappa}\left(\frac{\partial u}{\partial y}\right)^2-c_{\varepsilon_2}\rho\frac{\varepsilon^2}{\kappa} \quad (5)$$

According to the high Reynolds number (κ-ε) turbulence model the turbulent viscosity μ_t is related to the turbulent kinetic energy (κ) and to the dissipation of turbulent kinetic energy (ε) through the expression;

$$\mu_t = c_\mu \rho\frac{\kappa^2}{\varepsilon} \quad (6)$$

The effective viscosity (μ_{eff}) is related to the turbulent viscosity (μ_t) and to the molecular viscosity (μ) through the relation :-

$$\mu_{eff} = \mu_t + \mu \quad (7)$$

In the above equations, ($c_\mu, c_{\varepsilon_1}, c_{\varepsilon_2}\sigma_k, \sigma_\varepsilon$) are constants at high Reynolds number and the model constants $c_\mu, c_{\varepsilon 1}, c_{\varepsilon 2}$ are set to $c_\mu = 0.09, c_{\varepsilon 1} = 1.44, c_{\varepsilon 2} = 1.92$. Usually, the constants $\sigma_k and \sigma_\varepsilon$ are assigned to $\sigma_k = 1.0 and \sigma_\varepsilon = 1.3$.

The energy equation is;

$$\rho\, cp\left(\frac{\partial T}{\partial t}+u\frac{\partial T}{\partial x}+v\frac{\partial T}{\partial y}\right)=\frac{\partial}{\partial y}\left(k\frac{\partial T}{\partial y}\right)+\frac{\partial}{\partial y}\left(k_t\frac{\partial T}{\partial Y}\right) \quad (8)$$

where;

$$k_t = \frac{\mu_t cp}{\mathrm{Pr}_t} \quad (9)$$

For the evaluation of turbulent kinetic energy and dissipation at turbulent Kinetic energy, it is sufficed to fix their values at the near wall node (P) according to the following formula:-

$$\kappa_{\mathrm{P}} = \frac{\tau_\omega}{\rho c_\mu^{1/2}} \quad (10)$$

$$\varepsilon_{\mathrm{P}} = \frac{c_\mu^{3/4}}{V_K y_{\mathrm{P}}}\kappa_{\mathrm{P}}^{3/2} \quad (11)$$

$$y^+ = \frac{\rho y_p c_\mu^{1/4} k_p^{1/2}}{\mu_l} \quad (12)$$

where (y_p)is the normal distance of the near wall node (p) to the solid surface. In the above formula, (k) is the Von Karman constant (0.4187) and (E) is an integration constant that depends on the roughness of the wall. For a smooth wall constant shear stress, (E) has a value of (9.793).

The initial and Boundary conditions for the problem are shown to in **Fig.2**. all the previously discussed differential equations can be conveniently presented in the general form:-

$$\frac{\partial}{\partial t}(\rho\phi)+\frac{\partial}{\partial x}(\rho u\phi)+\frac{\partial}{\partial y}(\rho v\phi)-\frac{\partial}{\partial x}\left[\Gamma_\phi\frac{\partial\phi}{\partial x}\right]-\frac{\partial}{\partial y}\left[\Gamma_\phi\frac{\partial\phi}{\partial y}\right]=s_\phi \qquad (13)$$

In the above equation, ϕ identifies the dependent variables, Γ_ϕ is the appropriate exchange coefficient for the variable ϕ, and s_ϕ is the source term which includes both the sources of ϕ (positive or negative) and any other terms which cannot find place on the left-hand side of **Eq.(13)**, see **Table .2** .

The derived governing equations and the initial and boundary conditions in **Fig.2** Will be solved numerically by using the control volume approach of **(Patanker 1980)**. The finite difference method (F.D.M.) will be used, and the details of the numerical solution will be described in the next article.

NUMRICAL SOLUTION:-

The general from **Eq.(13)** may be written as;

$$\frac{\partial}{\partial t}(\rho\Phi)+\frac{\partial}{\partial x}\left[\rho u\phi-\Gamma_\Phi\frac{d\phi}{dx}\right]+\frac{\partial}{\partial y}\left[\rho v\phi-\Gamma_\Phi\frac{d\phi}{dx}\right]=S_\Phi \qquad (14)$$

By defining Jas the total flux which consists of convection and diffusion fluxes, or

$$J_x=\rho u\phi-\Gamma\frac{\partial\phi}{\partial x} \qquad (15)$$

$$J_y=\rho v\phi-\Gamma\frac{\partial\phi}{\partial y} \qquad (16)$$

Where J_x and J_Y or the total fluxes through faces normal to the x and y directions respectively with these definitions, **Eq. (14)** can be written

$$\frac{\partial}{\partial t}(\rho\phi)+\frac{\partial J_x}{\partial x}+\frac{\partial J_y}{\partial y}=S_\Phi \qquad (17)$$

Eq. (17) was integrated by using the finite volume approach of **(Patenker 1980)**, see **Fig. 3**. The source term has been linerized, and the values at the control volume faces (e, w, n, s) are assumed to be found by linear interpolation (central differences). The resulting final form of the **Eq. (17)** becomes

$$\frac{\left(\rho\mathrm{P}\phi_\mathrm{P}-\rho\mathrm{P}^\circ\phi_\mathrm{P}\right)\Delta x\Delta y}{\Delta t}+J_e-J_w+J_n-J_S=\left(S_c+S_\mathrm{P}\phi_\mathrm{P}\right)\Delta x\Delta y \qquad (18)$$

$$a_\mathrm{P}\phi_\mathrm{P}=a_E\phi_E+a_W\phi_W+a_N\phi_N+a_S\phi_S+b$$

$$a_E=D_eA(\mathrm{P}_e)+Max[-F_e,o]$$

$$a_W=D_wA(\mathrm{P}_w)+Max[F_w,0] \qquad (19)$$

$$a_N = D_n A(\mathrm{P}_n) + Max[-F_n, 0]$$
$$a_S = D_S A(\mathrm{P}_S) + Max[F_S, 0]$$
$$a_{\mathrm{P}}^{\circ} = \frac{\rho_{\mathrm{P}}^{\circ} \Delta x \Delta y}{\Delta t} \qquad b = S_c \Delta x \Delta y + a_{\mathrm{P}}^{\circ} \phi_{\mathrm{P}}^{\circ} \qquad (20)$$
$$a_{\mathrm{P}} = a_E + a_W + a_N + a_S + a_{\mathrm{P}}^{\circ} - S_{\mathrm{P}} \Delta x \Delta y \qquad (21)$$
$$\begin{aligned} \phi_e &= \phi_E f_e + \phi_p [1 - f_e] \\ \phi_w &= \phi_W f_w + \phi_p [1 - f_w] \\ \phi_n &= \phi_N f_n + \phi_p [1 - f_n] \\ \phi s &= \phi_S f_s + \phi_p [1 - f_s] \end{aligned} \qquad (22)$$

Generally

$$a_{\mathrm{P}} \phi_{\mathrm{P}} = \sum_{nb} a_{nb} \phi_{nb} + b \qquad nb = E, W, N, S \qquad (23)$$

where: b = Absolute part of the discretized equation

RESULTS AND DISUSION:-

The investigated case was the flow over a flat plate (1m) length. The height of the calculation domain was taken to be (0.03m), which was twice the boundary layer thickness at the trailing edge. The flow conditions were chosen to ensure that the flow is compressible and turbulent. The free stream pressure and temperature was taken as (101325 pa and 25 $^{\circ}$c). The Mach number was taken as (0.5). Accordingly, the free stream velocity was calculated as (156 m/s). The Reynolds number was calculated to be (1.02E+7). The suction and injection rates were taken as [±0.001 and ±0.0005 (+for injection and – suction)] of the free stream velocity. The wall temperature was taken as (70 $^{\circ}$c).The results will be shown for the solid wall and porous wall with injection and suction, but since the rate of injection and suction were small, their effects are not clear in the figures

Steady State Results:-

Fig.4 to **6** show the velocity profiles with injection or suction. The relative shapes for the velocity profiles are turbulent in these figures. The turbulent profile has apportioned near the wall which is almost linear. This portion is due to a laminar sub layer which hugs the surface very closely. Outside this sublayer the velocity profile is relatively flat in comparison with the laminar profile. It can be concluded from these figures, that injection causes a decrease in boundary layer thickness, while suction causes an increase in boundary layer thickness, and the rate of increase or decrease is proportional to the injection or suction rate, respectively. **Fig.7** to **9** show the temperature distributions inside the thermal boundary-layer with and without injection or suction. The very steep temperature gradient near the wall and the flatness of the profiles indicate clearly the turbulent shape of the profiles. Injection causes a slight decrease in temperature while suction causes reverse effect. **Fig.10** and **11** show the local skin-friction coefficient and the local Nusselt number coefficient respectively, with and without injection or suction. The skin friction coefficient decreases with the flow direction (increasing Rex) due to the decrease of the velocity gradient at the wall, which is caused by the decrease of the velocity of points near the wall due to the increase in resisting viscous forces. This happens for all cases, with and without injection or suction. The injection or suction causes slight difference due to small rates of injection and suction used. But, it can be noticed that injection causes a decrease in (cf_x), while suction causes reverse effect. **Fig.11**

and **13** show the hydrodynamic and thermal boundary-layer growth with and without injection or suction. **Fig.12** shows a decrease in the hydrodynamic boundary-layer thickness with injection. This is so because injection causes an increase in the velocity for points near the wall, which decrease the boundary-layer thickness. The boundary-layer, evidently, begins to grow from zero thickness at the leading edge and continues downstream tending asymptotically to the value given by the equation:-

$$\delta = \frac{0.376x}{\mathrm{Re}_x^{0.2}}$$

Fig.13 indicates an increase in thermal boundary-layer thickness with injection and a decrease with suction.

Transient Results:-

Fig.14 to **16** show the boundary-layer velocity profile history at the trailing edge with and without injection and suction. The time required to reach the steady state is found to be (4.4s) for the solid wall case (V_w=0 m/s). Injection causes an increase of this time to (V_w=0.156m/s). Suction causes reverse effect, that it decreases this time to (2.8s) for (V_w=-0.078m/s) and (1.4s) for (V_w=-0.156m/s). These effects are due to the disturbances caused by injection or suction to or from the boundary-layer. **Fig.17** to **19** show the temperature history across the thermal boundary-layer with and without injection or suction. The temperature profiles consist of linear part near the wall, superimposed on it a parabolic profile due to heat generated by friction. In an analogous way similar to that in **Figs. 14** to **16**, the time required to reach the steady temperature profiles is found to be the (4.2s) for the solid wall (V_w=0), (2.8s) for (V_w=-0.078m/s) and (1s) for (V_w=-0.156m/s). **Fig.20** and **21** show the hydrodynamic and thermal boundary-layers history at the trailing edge. The figures indicate in a very clear picture the effects of injection or suction on the time required to reach the steady state case, which is mentioned and discussed above .The values of this time differ slightly in this case, as shown in **Table.1**. **Fig.22** and **23** show the variation of the average skin friction coefficient and Nusselt number with time. The figures demonstrates the increase of the steady state time with injection and decrease with suction see **Table.2**. **Fig.24** and **25** show the comparison between the empirical and the numerical values of boundary-layer thickness and the local Nusselt number. The maximum relative difference on this line was (18.5%) for the boundary-layer thickness and (26.7%) for the Nusselt number. The minimum relative difference is (1.6%) for the boundary-layer thickness, and (18.28%) for the Nusselt number. The average relative difference is (12.7%) for the boundary layer thickness, and (21.28%) for the Nusselt number.

CONCLUSIONS

Injection causes a slight decrease in the temperature inside the thermal boundary-layer, while suction causes reverse effect. Turbulence kinetic energy level decreases away from the wall region, while effective viscosity level increases away from the walls region. The dissipation rate of turbulence is maximum at points adjacent to the wall surface where the velocity is in the minimum values. The local skin friction coefficient decreases with the flow direction. It can be noticed that injection causes a decrease in local skin friction coefficient while suction causes reverse effect. The local Nusselt number increases with local Reynold number, despite that the local heat transfer coefficient (h_x) decreases with the flow direction due to the increase in the thermal boundary layer

thickness. Injection causes a slight increase in Nusselt number and suction causes reverse effect. The hydrodynamic boundary layer thickness decrease with injection, while thermal boundary layer thickness increases with injection. Injection causes an increase in the time required to reach the steady state, while suction causes a reverse effect.

Table.1: Steady State Time for (δ_h) and (δ_t)

V_w(m/s)	Time (s)	
	δ_h	δ_t
0(solid wall)	4.2	4.2
0.078(injection)	5.5	5.7
0.156(injection)	6.7	6.7
-0.078(suction)	2.7	2.8
-0.156(suction)	1	1

Table.2: Steady State Time for ($\overline{c_f}$) and ($\overline{Nu}$)

V_w(m/s)	Time (s)	
	$\overline{c_f}$	$\overline{Nu}$
0(solid wall)	4.1	3.9
0.078(injection)	5.1	5.5
0.156(injection)	6.4	6.6
-0.078(suction)	2.3	2.5
-0.156(suction)	1.1	2.5

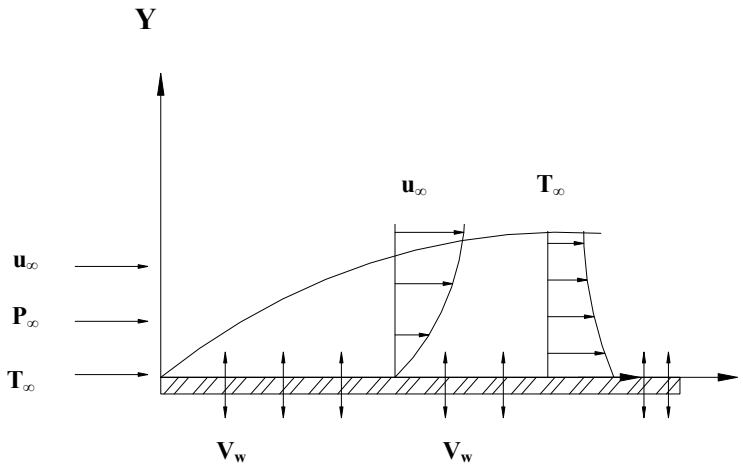

Fig.1: The Problem of the Present Work

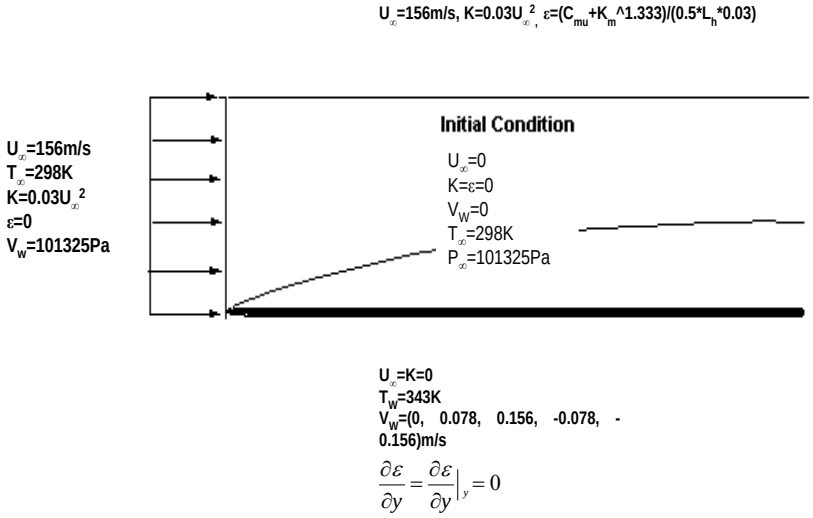

Fig.2: The Initial and Boundary Condition

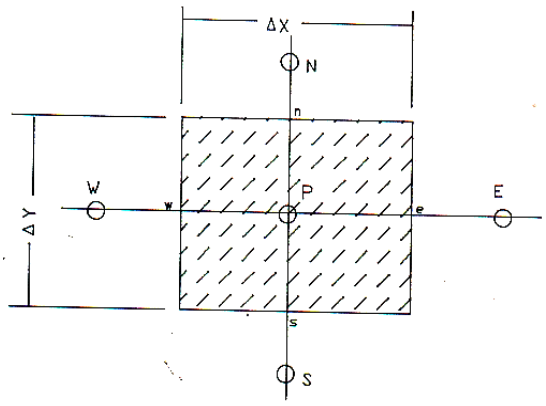

Fig. 3: Control Volume for Tow- Dimensional Case

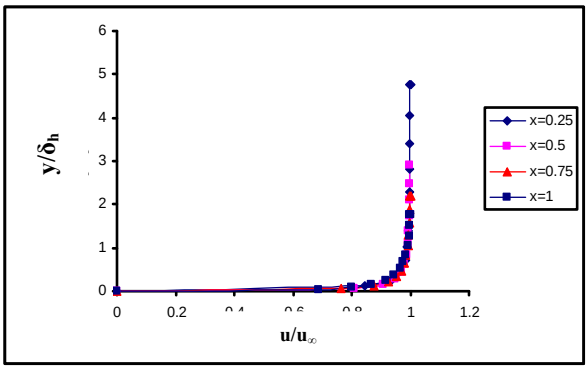

Fig. 4: Boundary-Layer Velocity Profiles (V_w=0m/s)

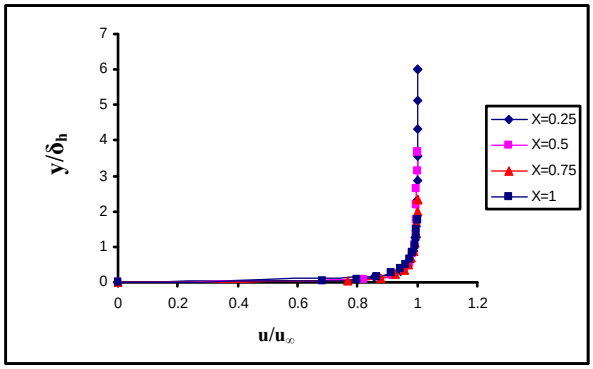

Fig. 5: Boundary-Layer Velocity Profiles (V_w=0.156m/s)

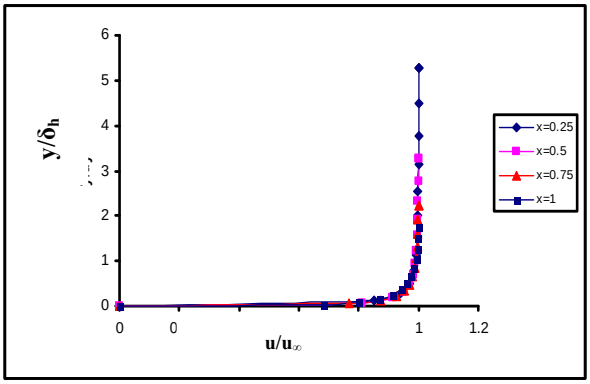

Fig. 6: Boundary-Layer Velocity Profiles (V_w=0.156m/s)

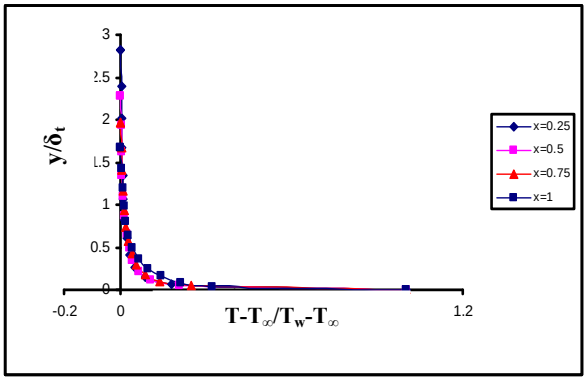

Fig. 7: Thermal Boundary-Layer Temperature Profiles (V_w=0m/s)

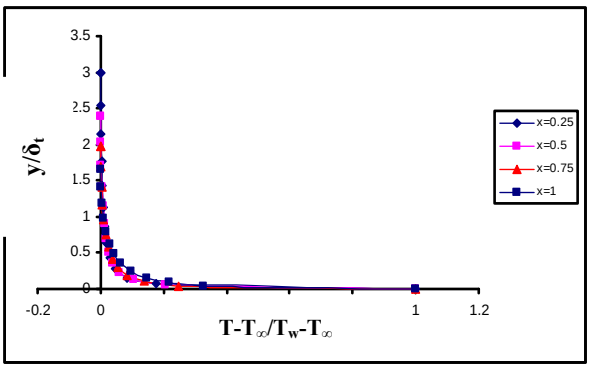

Fig. 8: Thermal Boundary-Layer Temperature Profiles (V_w=0m/s)

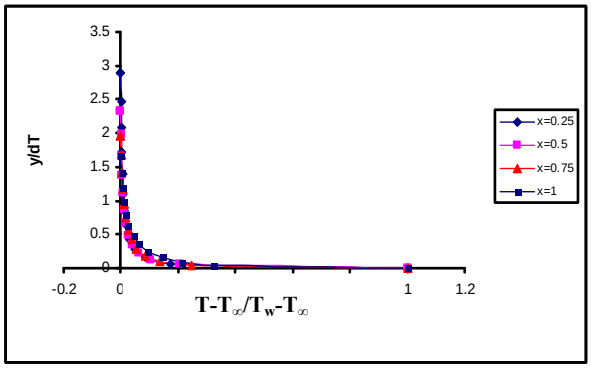

Fig. 9: Thermal Boundary-Layer Temperature Profiles (V_w=0m/s)

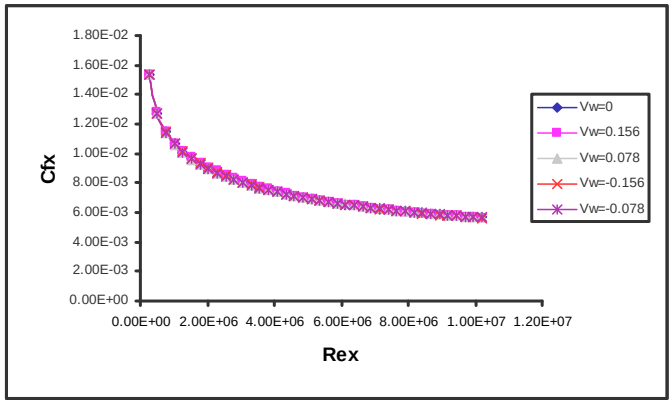

Fig. 10: Local skin Friction Coefficient Variation with Local Reynolds Number

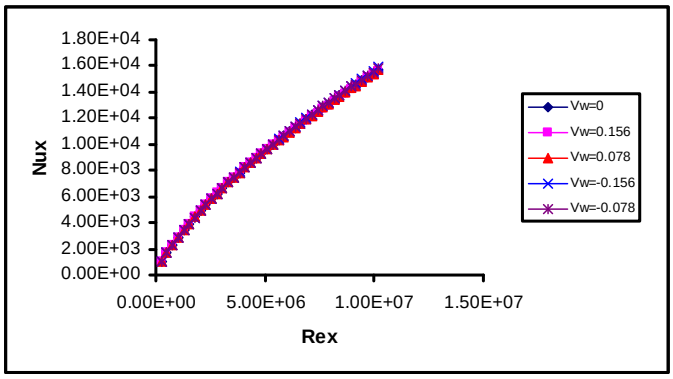

Fig. 11: Local Nusselt Number variation with local Reynolds Number

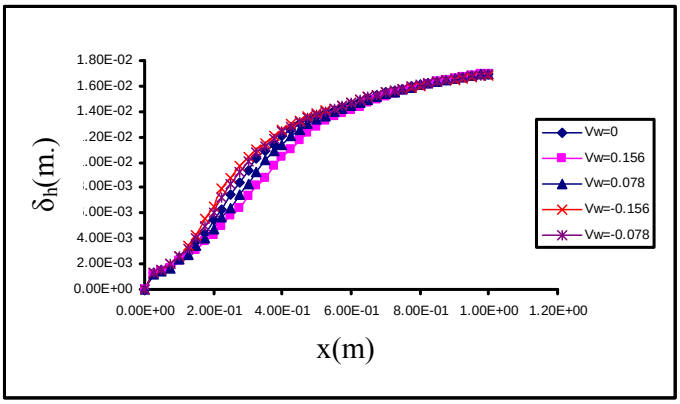

Fig. 12: Hydrodynamic Boundary-Layer Thickness Growth

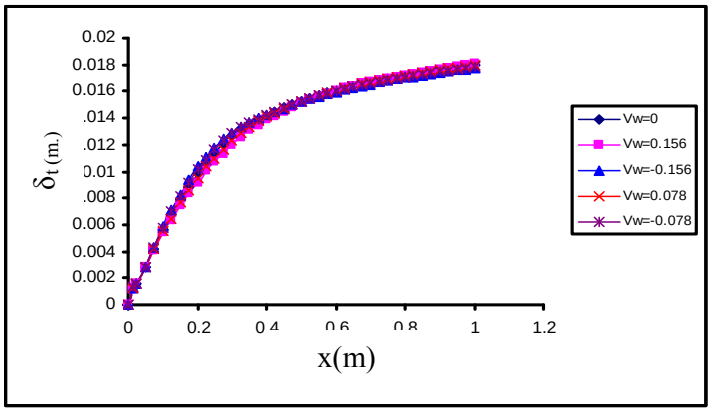

Fig. 13: Thermal Boundary-Layer Thickness Growth

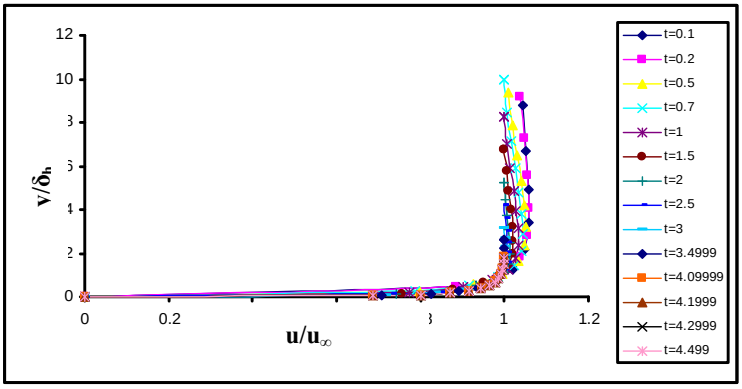

Fig. 14: Boundary-Layer Velocity Profile History at Trailing Edge (V_w=0m/s)

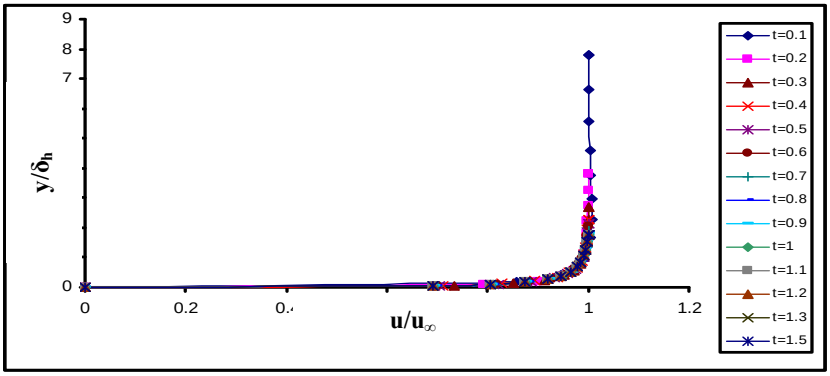

Fig. 15: Boundary-Layer Velocity Profile History at Trailing Edge (V_w=-0.156m/s)

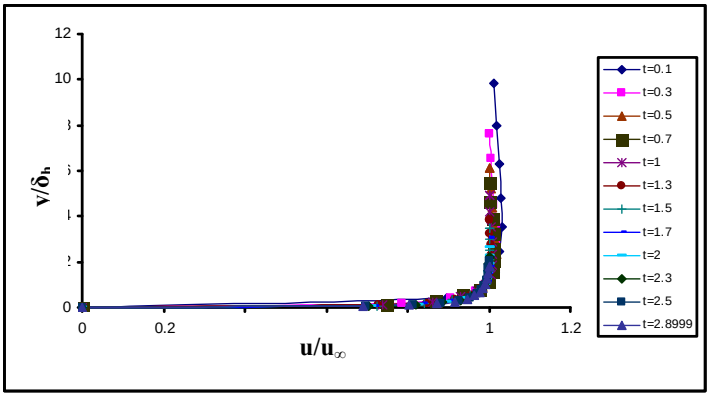

Fig. 16: Boundary-Layer Velocity Profile History at Trailing Edge (V_w=-0.078m/s)

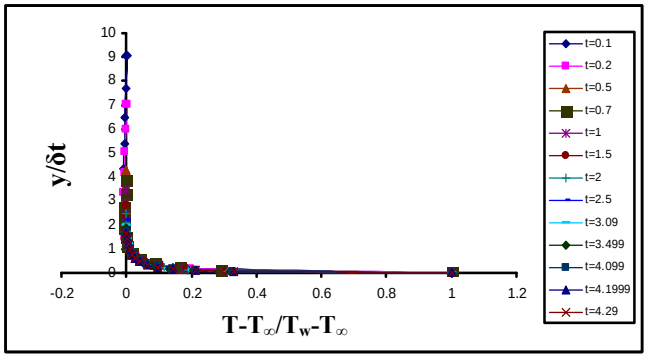

Fig. 17: Boundary-Layer Temperature Profile History at Trailing Edge (V_w=0m/s)

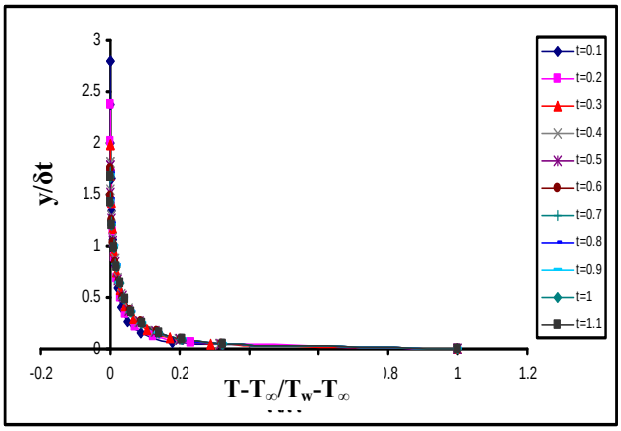

Fig. 18: Boundary-Layer Temperature Profile History at Trailing Edge (V_w=-0.156m/s)

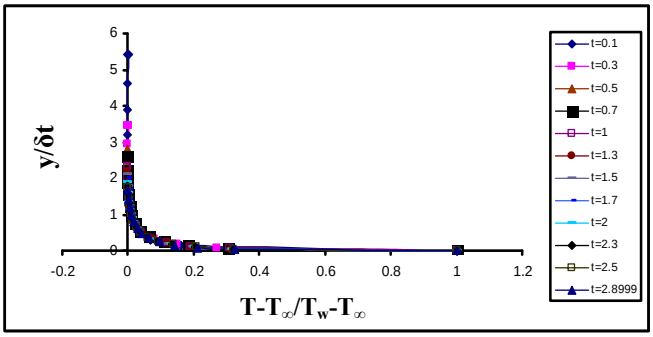

Fig. 19: Boundary-Layer Temperature Profile History at Trailing Edge (V_w=-0.078m/s)

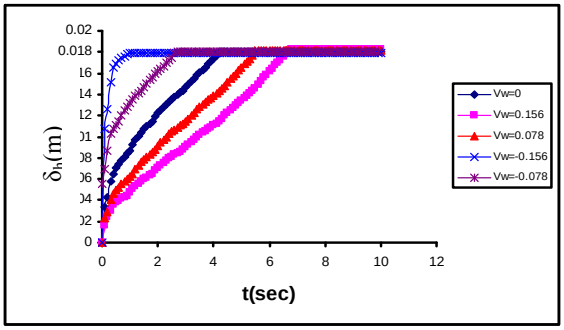

Fig.20: Hydrodynamic Boundary-Layer Variation with Time

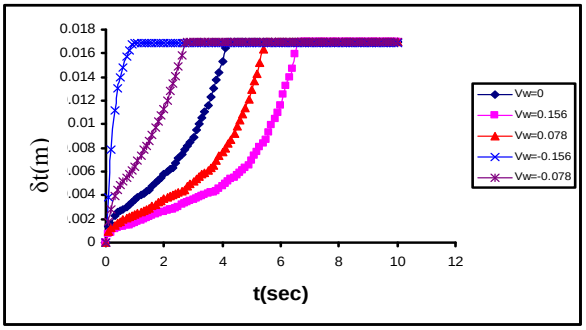

Fig. 21: Temperature Boundary-Layer Variation with Time

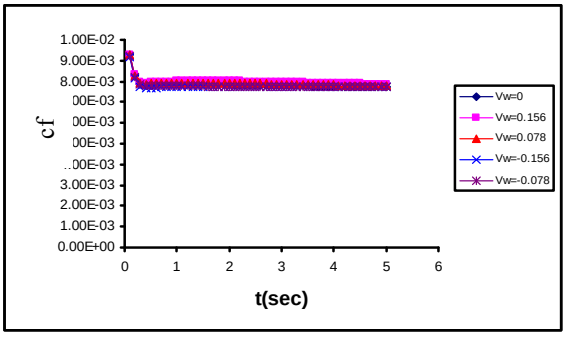

Fig. 22: Mean Skin Friction Variation with Time

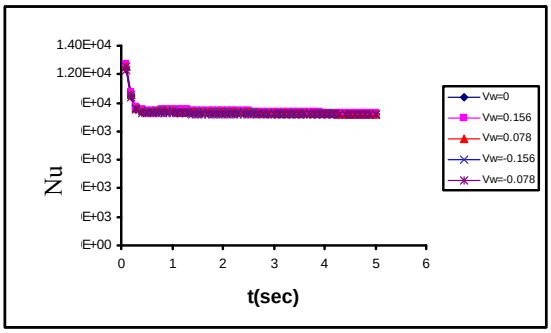

Fig. 23: Mean Nusselt Number Variation with Time

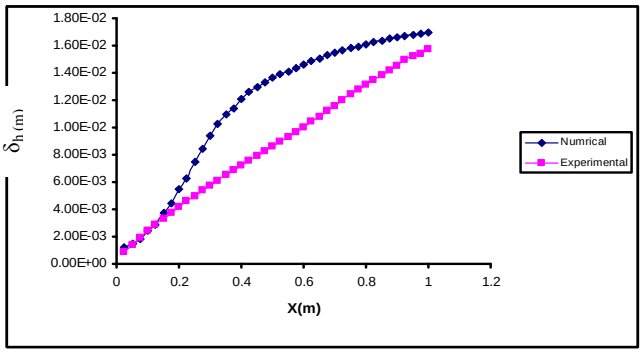

Fig. 24: Comparison of Hydrodynamic Boundary-Layer Results

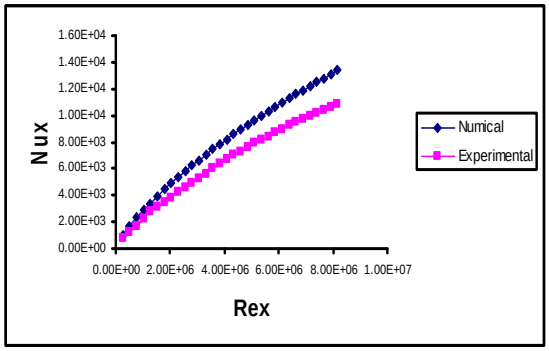

Fig. 25: Comparison of Nusselt Number Results

REFFRENCES

Ayser M. Fleh " Unsteady Hydrodynamic and Thermal Boundary Layers over a Porous Flat Plate", M.Sc. Thesis, Mech. Eng. Dept., University of Al-Mustansirya, 2005

Jeongyoung P. and Haecheon C., "Effects of Uniform or Suction From a Spanwise Slot on a Turbulent Boundary-Layer Flow" J. Physics of Fluids, Vol.11, No. 10, PP. 3095-3105, October (1999).

Kyoungyoun K. and Hyung J. "Assessment of Local Blowing and in a Turbulent Boundary-Layer" Fluid Mechanics Conference Adelaide University, PP. 215-218, December (2001).

Kyoungyoun K. and Hyung J. "Effects of Periodic Blowing from Spanwise Slot on a Turbulent Boundary-Layer" AIAA Journal, Vol.41, No. 10, PP.1916-1924, October (2003).

Nagano Y. and Hishida M., "Improved Form of the $\kappa - \varepsilon$ Model for Wall Turbulent Shear Flows " J. Fluid Mech., Vol.109, PP. 156-160, June (1987).

Nagano Y. and Hishida M., "An Improved $\kappa - \varepsilon$ Model for Boundary Layer Flows " J. Fluid Mech., vol. 112, PP. 33-39, March (1990).

Park, S.H. and Sung, H.J. "Effect of Local Forcing on a Turbulent Boundary Layer" J.Experiments in Fluids, 31, pp 384-393, 2001

Patanker, S.V. " Numerical Heat Transfer and Fluid Flow ", McGraw-Hill Book Company, 1980

Per-Age K. and Anatoli K., "Some Effects of Localized Injection on the Turbulence Structure in a Boundary-layer" J. Physics of Fluids, Vol. 12, No. 11, PP. 2990-2998, November (2000).

NOMENCLATUR

Latin Symbols

Symbol	Description	Units
C_{f_x}	Local Skin-Friction Coefficient	
C_P	Pressure Coefficient, also the Specific Heat at Constant Pressure	J/kg. K
E, W, N, S	Nodal Points Neighbor (Refer to East, West, North and South)	
F	Convective Flux Through a cell Face	m^2/s
J	Flux	$kg/m\ s^2$
K	Thermal Conductivity	W/m. k
K	Kinetic Energy of Turbulence	J
K	Ratio of Specific's Heat, (=1.4 for air)	
M	Molecular Weight	kg/mol
M	Mach number	
Nu	Nusselt Number	
P	Pressure	N/m^2
P	Cell Nodal Point	
Pr	Prandtl Number	
R_e	Reynolds Number	
S	Source Term	
S_R	Sum of Residuals	
T	Temperature	
T_w	the Wall Temperature	
t	Time	sec
U	The Velocity Vector	m/sec
u, v, w	Velocity Components in the x, y and z	m/sec
X, x	X-Coordinate Distance	m
Y, y	Y-Coordinate Distance	m

GREEK SYMBOLS

Symbol	Description	Units
α	Under-relaxation Factor	
ε	Dissipation Rate of Turbulent	
$\Delta X, \Delta Y, \Delta Z$	Cell Distances	
$\delta k, \delta \varepsilon$	Constant in the $K-\varepsilon$ Model	
$\delta x, \delta y$	Half the Cell Distances	
δh	Hydrodynamic Boundary-Layer Thickness	m
δt	Thermal Boundary-Layer Thickness m	
Φ	Dependent Variable in the General Form of Equation	
Γ	Transfer Coefficient	

Γ_{wall}	Diffusion at the Wall	
μ	Laminar Viscosity	kg/m.s
μ_{eff}	Effective Eddy Viscosity	kg/m.s
ρ	Density kg/m^3	
ρ_{sea}	Sea Level Density, (=1.225 Kg/m^3)	kg/m^3
ν	Kinematics Viscosity	m^2/s
$\tau_w, \tau_\circ$	Wall Shear Stress	N/m^2

SUBSCRIPTS

Symbol	Description	Units
e, w, n, s	At The Center of The Cell Face	
i, j, k	Coordinate Direction Indices	
nb	Neighbor Points	
o	Initial Value	
P, E, W, N, S	of the Nodal Point	

SUPERSCRIPTS

Symbol	Description
o	Old Values
∞	Signifies Free Stream Conditions